Smart Materials in Medicine 3 (2022) 289–296

Contents lists available at ScienceDirect

Smart Materials in Medicine

journal homepage: www.keaipublishing.com/en/journals/smart-materials-in-medicine/

Phoxim-specific DNA aptamer screening, characterization and application in a multiple complementary strands fluorescent aptasensor

Wenfei Guo [a], Dan Wei [a], Franklin Wang-Ngai Chow [b], Polly Hang-Mei Leung [b], Hanming Wang [c], Lei Cai [d], Masahi Hori [e], Zhu Chen [a], Song Li [a,*], Yan Deng [a,**]

[a] Hunan Key Laboratory of Biomedical Nanomaterials and Devices, Hunan University of Technology, Zhuzhou, 412007, PR China
[b] Department of Health Technology and Informatics, The Hong Kong Polytechnic University, Hong Kong, 999077, PR China
[c] Guangzhou Wondfo Biotech Co., Ltd., Guangzhou, 510663, PR China
[d] Guangzhou Wondfo iCubate Biotech Co., Ltd, Guangzhou, 510641, PR China
[e] FNW Inc, Tokyo, 135-0051, Japan

ARTICLE INFO

Keywords:
Aptamer
Fluorescence aptasensor
SELEX
Phoxim
Detection

ABSTRACT

In order to develop a fluorometric aptamer-based biosensor for ultrasensitive and selective detection of phoxim, a modified magnetic beads-systematic evolution of ligands by exponential enrichment (MB-SELEX) method was used in this study to select phoxim aptamer. An aptamer (APT3) that bonded to phoxim with high affinity was obtained after 15 rounds of selection, which had dissociation constant (K_d) of 0.93 ± 0.25 μM. A fluorometric aptasensor was then developed and enhanced the sensitivity and selectivity of phoxim detection based on APT3, multi-complementary strands (CS) and gold nanoparticles (AuNPs). This method had a good linear range of 0.05–5 μM, and detection limit was as low as 29.69 nM for phoxim. In addition, the aptasensing specifically captured phoxim in a variety of pesticides and real samples. The herein results proved that the method can be applied in practical detection.

1. Introduction

Phoxim is a widely used organophosphorus insecticide that is suitable for a variety of Lepidoptera pests with high lethality [1]. Currently, phoxim is widely used for pest control in crops, however, it can enter the human body through inhalation, ingestion and percutaneous absorption [2–4]. Long-term accumulation of phoxim will lead to diseases, cancer and even poisonous death, affecting the next generation, and posing a threat to human health and environment [5,6].

The current methods for determination of phoxim include high performance liquid chromatography (HPLC), gas chromatography/mass spectrum (GC/MS), thin-layer chromatography (TLC), liquid chromatography-tandem mass spectrometry (LC/MS) and so on [7]. These methods take a long time and high cost, and usually require complex sample pretreatment, expensive instruments and professional operators, so it is difficult to apply in field detection. The reported sensors for phoxim detection are mainly based on polymer materials and enzymes. Molecularly imprinted sensor based on polymer materials has high sensitivity, but it has low specificity and accuracy to the target [8,9]. Enzyme inhibition method and enzyme-linked immunosorbent assay (ELISA) have fast reaction speed and high specificity [10,11], but preparation of enzyme is complex, easy to inactivate, differences between batches, and sensitive to environmental factors such as pH, temperature and UV irradiation, which affect the accuracy of the sensor [12]. Functional nucleic acids play an important role in molecular detection [13–15].

Aptamers, also known as artificial antibodies, are short single-stranded DNA or RNA molecules obtained by systematic evolution of ligands by enrichment (SELEX) [16–19]. Compared with traditional antibodies, aptamers have advantages, such as simple preparation, good stability, easy labeling, strong specificity and high affinity [20,21]. At present, aptamers have been widely used in the detection of cells, viruses, proteins, sugars, metals and pesticides [22,23]. The fluorescence sensor has the advantages, such as high sensitivity, fast reaction speed, convenient operation and so on [24–26]. In recent years, reports on pesticide aptamer sensors have gradually increased [27,28]. For example, Hong and Cooter [29] obtained an aptamer of fipronil (K_d = 48 ± 8 nM) and constructed a fluorescent aptasensor with a detection limit of 105 nM in

* Corresponding author.
** Corresponding author.
E-mail addresses: solisong@163.com (S. Li), hndengyan@126.com (Y. Deng).

https://doi.org/10.1016/j.smaim.2022.03.003
Received 8 January 2022; Received in revised form 18 March 2022; Accepted 18 March 2022
Available online 22 March 2022

river water. Liu et al. [30] selected an aptamer of carbaryl with K_d = 0.364 ± 0.055 μM by ssDNA library immobilized SELEX method, and constructed a fluorescent aptasensor with high sensitivity, and the limit of detection (LOD) was as low as 15.23 nM.

The traditional fluorescence aptasensor with competitive binding aptamer between target and complementary strand (CS) have characteristics of having single binding site and low molecular weight because of their small molecular targets, and the binding with aptamer is easy to be disturbed by steric hindrance and environmental factors. It is also difficult to fully combine with the aptamer, which greatly affects the accuracy of the sensor. How to construct a fluorescent aptasensor which can capture small molecular targets stably and sensitively is a research hotspot in recent years. Bahreyni et al. [31] designed a multiple complementary strands fluorescence sensor that could detect acetamiprid as low as 2.8 nM. The advantage of this sensor is that the target and aptamer are incubated preferentially in solution, which can reduce the influence of other sequences and environmental factors on it, allowing the target to be fully captured by the aptamer [32]. Secondly, because AuNPs can strongly quench fluorescence through nanometal surface energy transfer (NSET), the background signal of the sensor is weakened and sensitivity of the sensor is improved [33,34].

In this study, we used magnetic beads-SELEX (MB-SELEX) technique to select aptamer for phoxim, and quantitative polymerase chain reaction (Q-PCR) amplification curve-melting curve analysis (AC-MCA) was used to monitor the selection process. Following, a fluorescent aptasensor with multi-complementary strands structure using AuNPs as quenching agent was fabricated, and the sensor was used to capture phoxim in real samples. The sensor retains the original structure of the aptamer and has the advantages of stable structure, low background signal and good repeatability, so it is more suitable for the detection of small molecular targets.

2. Materials and methods

2.1. Materials and instruments

Phoxim and other pesticides were purchased from Tanmo Quality of science and technology Co., Ltd. (Changzhou, China). Streptavidin coated magnetic beads were purchased from Beaver Biosciences Inc. (Suzhou, China). Emulsion PCR (ePCR) microdroplet generation oil and 3.5 KD dialysis membrane were purchased from Anhui Aptamy Biotechnology Co., Ltd. (Hefei, China). Nano gold colloid was purchased from Jiangsu XFNANO Materials Tech. Co., Ltd. (Nanjing, China). Taq PCR Master Mix and Taq Q-PCR mix was purchased from Vazyme Biotechnology Co., Ltd. (Nanjing, China). DPBS solution consisted of the following components: NaCl 136.89 mM, KCl 2.67 mM, Na_2HPO_4 8.10 mM, KH_2PO_4 1.47 mM. In this experiment, all the oligonucleotides were synthesized and HPLC-purified by Sangon Biotechnology. (Shanghai, China). The sequence information is shown in Table 1.

PCR experiment reaction was carried in T-100 thermal cycler. (Bio-rad, USA). Q-PCR experiment was carried out in Light Cycler®96 instrument. (Roche, Switzerland). A Hitachi F-7100 fluorescence spectrometer (Hitachi, Japan) was used to record the fluorescence intensity, with an excited slit and emission slit of 5.0 nm.

2.2. Selection procedure

In brief, the selection of phoxim by MB-SELEX included library hybridization, immobilization, elution, amplification and purification. The selection process is shown in Scheme 1a. The entire selection process was quantified by Q-PCR, and was monitored by AC-MAC method.

The initial library was injected at 1 OD, and the Lib-biotin was added at the molar ratio of 1:2. The mixture was placed in the PCR instrument at 95 °C for 1 min, 59 °C for 60 min, and 25 °C for 10 min. The cooling rate between 59 °C and 25 °C was 0.1 °C/s. The concentration was measured by trace ultraviolet OD instrument and recorded as C1. Magnetic beads and hybridization library were incubated in the shaker for 50 min. The supernatant was then separated on the magnetic separation rack, and the concentration of ssDNA in the solution was measured by trace ultraviolet OD instrument, which was recorded as C2. Subsequently, 100 μM phoxim was added and incubated with the beads for 50 min, and the eluent with affinity for phoxim was obtained and recorded as E. The phoxim in the eluate was removed by a dialysis device. The input amount of the library in subsequent rounds was kept at 0.15 nmol. The amounts of Lib-biotin and magnetic beads were reduced to 0.3 nmol and 100 μL, respectively. The target concentration for each round is shown in Table 2. In order to improve the specificity of selection, the counter selection was added from 11th round, and concentration of counter selection pesticides increased gradually. The counter selection solution included omethoate, parathion, chlorpyrifos, dichlorvos and methyl parathion.

The eluent was enriched by ePCR, which maintained the diversity of the library and avoided amplification preference. 1 mL Taq PCR mix, 100 μL Lib-FAM (10 μM) and 100 μL Lib-polyA (10 μM) were added to the eluent and made up to 2 mL with ddH_2O and mixed for 2 min. The ePCR mixture was mixed with 8 mL ePCR microdroplet generation oil and shaken for 10 min to form a uniform white emulsion. The emulsion was packed into 96 tubes and put into the PCR instrument. The procedure was as follows: 95 °C for 3 min, followed by 23 cycles of 95 °C for 30 s, 60 °C for 30 s, 72 °C for 60 s and extended at 72 °C for 4 min. The enriched emulsion was concentrated to 100 μL by n-butanol.

The ssDNA library was prepared and recovered by urea-polyacrylamide gel electrophoresis (PAGE). 7 M urea-PAGE was composed of the following components: 3.78 g urea, 1.8 mL 40% Acryl/Bis solution, 1.8 mL 5 × TBE, 2.25 mL ddH_2O, 50 μL 10% APS, and 10 μL TEMED. The enriched library was mixed with 2 × loading buffer at the ratio of 1:1.5, and then 95 °C for 10 min, followed by freezing for 2 min. Electrophoresis was carried out at 350 V for 30 min, and then the fluorescence band was cut and moved to a centrifuge tube. 1 mL DPBS was added and heated at 95 °C for 10 min to transfer ssDNA into the solution. The ssDNA was purified using purification kit as the ssDNA pool for next round of selection.

In this experiment, Q-PCR was used to monitor the selection process. Q-PCR system was set as follows: 10 μL Q-PCR mix, 6.8 μL ddH_2O, 1.2 μL

Table 1
All oligonucleotide sequences in the screening process and sensors.

Name	Sequence (5'to3′)
Initial library	TCCAGCACTCCACGCATAACN(40)GTTATGCGTGCGACGGTGAA
LibF	TCCAGCACTCCACGCATAAC
LibR	TTCACCGTCGCACGCATAAC
Lib-biotin	GTTATGCGTGGAGTGCTGGA-Biotin
Lib-polyA	AAAAAAAAAAAAAAAAAAAAAAAAA/iSp18/TTCACCGTCGCACGCATAAC
Lib-FAM	FAM-TCCAGCACTCCACGCATAAC
APT3	TCCAGCACTCCACGCATAACGGCAGGAAGAGTAGTGATGAGTGGTGTTATGCGGGGTGTGGTTATGCGTGCGACGGTGAA
APT3s	CTCAGTCGCTCACTCCACGCATAACGGCAGGAAGAGTAGTGATGAGTGGTGTTATGCGGGGTGTGAGCGA
CS1	TCGCTCACACCCCGCATAACACCACTCATCACTACTCTTCCTGCCGTTATGCGTGGAGTGAGCGACTGAG
CS2-SH	GTTATGCGGGGTGTGAGCGA-SH
CS3-FAM	FAM-TCGCTCACACCCCGCATAAC

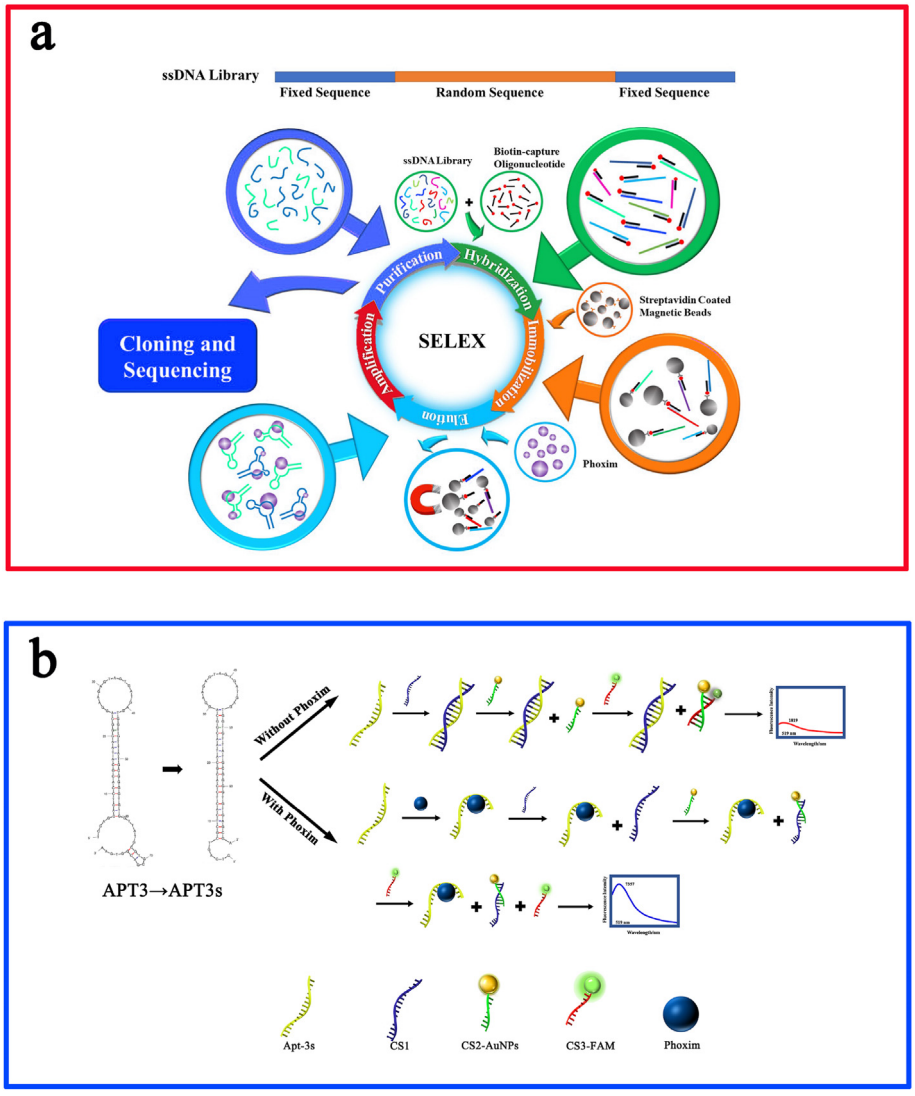

Scheme 1. (a) Schematic illustration of MB-SELEX process. (b) Illustration of fluorescent aptasensor with multiple complementary strands. In the absence of phoxim, CS2-AuNPs was bound to CS3-FAM and fluorescence signal was quenched. In the presence of phoxim, free CS3-FAM released fluorescence signal.

Table 2
The input amount of each substance in the selection process.

Selection round	Pool (nmol)	LibF1-biotin (nmol)	Magic beads (μL)	Phoxim (μM)	Negative pesticides (μM)
1	1.3	2.6	800	100	–
2	0.15	0.3	100	100	–
3	0.15	0.3	100	100	–
4	0.15	0.3	100	50	–
5	0.15	0.3	100	50	–
6	0.15	0.3	100	50	–
7	0.15	0.3	100	25	–
8	0.15	0.3	100	25	–
9	0.15	0.3	100	25	–
10	0.15	0.3	100	10	–
11	0.15	0.3	100	10	5
12	0.15	0.3	100	10	10
13	0.15	0.3	100	10	20
14	0.15	0.3	100	10	40
15	0.15	0.3	100	10	50

template, 1 μL LibF, and 1 μL LibR. The Cq value accurately quantified the concentration of ssDNA solution. Amplification Curve and Melting Curves Analysis (AC-MCA) were reflect the diversity in the library. When both curves remained stable, the selection was completed.

After 15 rounds of selection, AC-MCA double curve remained stable and the selection was completed. The library was sent to Sangon Biotechnology (Shanghai, China) for high-throughput sequencing. The results of high-throughput sequencing were shown in Table S1 (Support information). The results showed that the library obtained by screening was highly enriched, and only the first 15 of the more than 50000 sequences accounted for 12.76%. The secondary structure of the first 15 sequences were analyzed by M-Fold software and affinity of different sequences for phoxim was determined by following the hybridization, immobilization and elution steps in SELEX. 15 sequences of 0.15 nmol were fixed on magnetic beads and 100 μM phoxim was added for elution to obtain E_1-E_{15}. Each eluent was repeated in 3 groups, among which E_3 had the highest number of moles, which was named APT3.

2.3. *Design of multi-complementary strands fluorescent aptasensor*

APT3s was obtained by cutting and modifying APT3 to maintain the stem-loop structure and mismatch structure with recognition function. Complementary chains CS1, CS2-SH, and CS3-FAM were synthesized. Complementary chains were added to bind ssDNA in the solution after the aptamer were bound to phoxim, and the binding process is shown in Scheme 1b. Small molecular targets had characteristics, such as low

molecular weight, simple structure and single binding site, so the binding with aptamers was easily affected by steric hindrance and other factors [35]. By introducing multiple complementary strands into the sensor, their effect on the fluorescence signal due to insufficient binding of small molecules to the aptamer was reduced.

The extinction coefficient of AuNPs was higher than organic quenching groups, and G base exerted a quenching effect on fluorescence groups. Therefore, AuNPs modification on the G-rich CS2-SH sequence could achieve the best quenching effect. In order to activate the sulfhydryl groups, 15 μM CS2-SH was mixed with 1 M TECP solution for 30 min. To fabricate a sensitive aptasensor, the concentration ratio between AuNPs and CS2-SH was optimized. Firstly, 100 μM of activated CS2-SH was incubated with different concentration of AuNPs (50 μM–600 μM), respectively. As shown in Fig. S1 (Supporting information), the fluorescence intensity of CS3-FAM decreases along with the increase of its quenching strand. When the ratio increased to 3.5:1, the fluorescence intensity of FAM was almost quenched to minimum. Thus, the concentration ratio of 3.5:1 (AuNPs/CS2) was selected for further experiments. The activated CS2-SH was incubated with AuNPs (<10 nm) at the ratio of 3.5:1 for 48 h, and the CS2 was diluted to the final concentration of 0.5 μM to obtain CS2-AuNPs. Different concentrations of phoxim (0.01–60 μM) were incubated with 0.5 μM APT3s for 1 h to sufficient mixing. 0.5 μM CS1 was added and combined with APT3s, which did not bind to phoxim, and stabilized the APT3s-phoxim structure. Addition of CS2-AuNPs (0.5 μM) and complementary to CS1 was bound to CS1, which did not bound to aptamer and stabilized the APT3s-phoxim and CS1-APT3s structures. Finally, the CS3-FAM (0.5 μM) complementary to CS2 was added and combined with free CS2-AuNPs. The higher target concentration bound to the more aptamers resulted in the more free CS3-FAM and higher fluorescent signal. Conversely, the lower target concentration bound to the fewer the aptamers leaded to the more CS3-FAM bound to CS2-AuNPs, and the fluorescence signal was quenched. The fluorescence spectra were obtained by Hitachi F-7100 under excitation of 495 nm and an emission range from 507 to 600 nm. Each set of data measured contained five repetitive samples.

To verify the selectivity and usefulness of the sensor, the performance of the sensor was tested in other pesticides and real samples, respectively. The aptasensor was applied in the detection of a variety of pesticides, including 1-naphthol, omethoate, chlorothalonil, carbaryl, simazine, and paraquat. The structure of the pesticides were shown in Fig. S2 (Support information).

In order to validate and evaluate the accuracy as well as practical application of the constructed fluorescent aptasensor, the actual samples, which were collected from Xiangjiang River, were tested. The water samples were filtered with 0.22 μm microfiltration membrane to remove the solid impurities and suspension. A certain amount of phoxim standard solution was spiked into each river water sample with the final phoxim concentration 0.5 μM, 1.0 μM and 2.0 μM respectively. Then the concentration of phoxim was detected using this sensor.

3. Results and discussion

3.1. Selection of aptamers for phoxim

In this work, MB-SELEX was used to obtain phoxim aptamer, which was based on target-triggered release of ssDNA from the complex of ssDNA-capture oligonucleotide. It had the advantages of simple operation and short cycle, and was suitable for aptamer selection of small molecular targets. After 10 rounds of positive selection and 5 rounds of negative selection, nucleic acid sequences with affinity for phoxim were obtained. The addition of negative selection in the selection process reduced the effect of target analogues on selection and improved the specificity of selection. With progress of selection, the target concentration gradually decreased and the target analogue concentration was gradually increased, and the affinity of the library was also gradually increased.

The samples were purified and sent to Shanghai Sangon Biotechnology for high-throughput sequencing at the end of the selection. According to these results, the first 15 of more than 20000 sequences accounted for 15.76% of the total nucleic acid amount. The first 15 sequences were synthesized, and 0.15 nmol was immobilized on 100 μL magnetic beads, respectively, followed by elution with 100 μM phoxim. The elution amount is shown in Fig. 1. The third aptamer was synthesized and its secondary structure was predicted and named APT3. The stem-loop and mismatch structure were retained, sheared and modified to make its structure more stable, named APT3s.

3.2. Quantification and monitoring

During the selection process, we quantified the ssDNA solution and monitored their selection process by Q-PCR. Prior to selection, the library was diluted to 10 nM, 1n M, 0.1 nM, 0.1 nM, 0.01 nM, and 0.001 nM, respectively. Each concentration was repeated for 3 groups and the Q-PCR reaction was carried out, as shown in Fig. 2a. The linear fit was also performed for the number of cycles and logarithm of molecules amount to obtain the equation $Cq = -3.3687 \times \log N + 36.62$, N was the amount of ssDNA as shown in Fig. 2b. The library and eluent obtained by selection was accurately quantified by the linear equation. The libraries from each round of selection were carried on Q-PCR and obtained two sets of curves.: amplification curve and melting curve. The combination strategy proposed by Luo et al. [36] was proved to be a general and effective method for monitoring the selection process. In amplification curve (Fig. 2c), there was decreased in fluorescence in the first several rounds of SELEX. The explanation for this phenomenon is that the initial library contained a large number of random and non-specific ssDNA. The extension stage was limited by primers and dNTP in the later stage of PC, and oligonucleotide sequences mismatched and formed unstable hetero-duplex, resulting in decreased fluorescence. With progress of SELEX, the decreased fluorescence gradually disappeared, which also represented the decreased library diversity. In melting curve analysis (Fig. 2d) and melting peak at 82–87 °C increased gradually, and the melting peak at 70–72 °C also decreased gradually, which represented the gradual increase of homology in the library. After the 13th round of selection, the diversity of the library decreased gradually. The library diversity tended to be stable in the 14th and 15th rounds, so it was chosen to end the selection after the 15th round.

3.3. Construction of multi-complementary strands fluorescent aptasensor

As a small molecular target, phoxim was characterized with low molecular weight, simple structure and single binding site. The fluorescence aptasensor which destroyed the fluorescein-quenchant agent double strands by the target was susceptible to steric hindrance, incubation time and other environmental factors. In this sensor, the target was sufficiently mixed with the aptamer to form a stable target-aptamer structure. After addition of each complementary strands, it was bound to free sequence and stabilized the target-aptamer or dsDNA structure in the solution. The fluorescence sensor with multi-complementary strands structure can be widely used in small molecular targets.

According to results from the study, it was found that the G base in the sequence had obvious quenching effect on the FAM group. The fluorescence intensity of the modified FAM group on the G-rich ssDNA was significantly lower than that of the base-balanced FAM-ssDNA. In this work, according to characteristics of aptamers and CSs, the CS2 sequence contained 50% G bases, of which four G bases were adjacent. Therefore, the CS2 was decided to carry sulfhydryl group and AuNPs, so that the fluorescein on CS3 was doubly quenched by the AuNPs and G bases. The extinction coefficient of AuNPs was much higher than that of organic quenching agents [37]. The background signal for the fluorescence sensor was reduced and the sensitivity of the sensor was improved.

In the absence of the phoxim, the aptamer was fully mixed with CS1 in the solution, and CS2-AuNPs was mixed with CS3-FAM and the

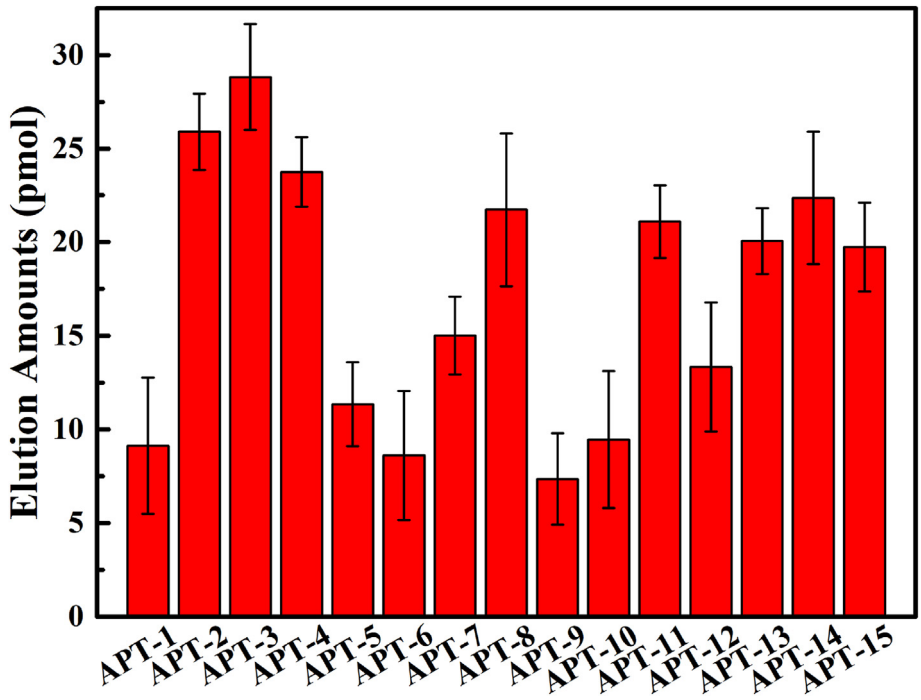

Fig. 1. The elution amount of ssDNA from 0.15 nmol different aptamer candidates incubated with 100 μM phoxim for 1 h.

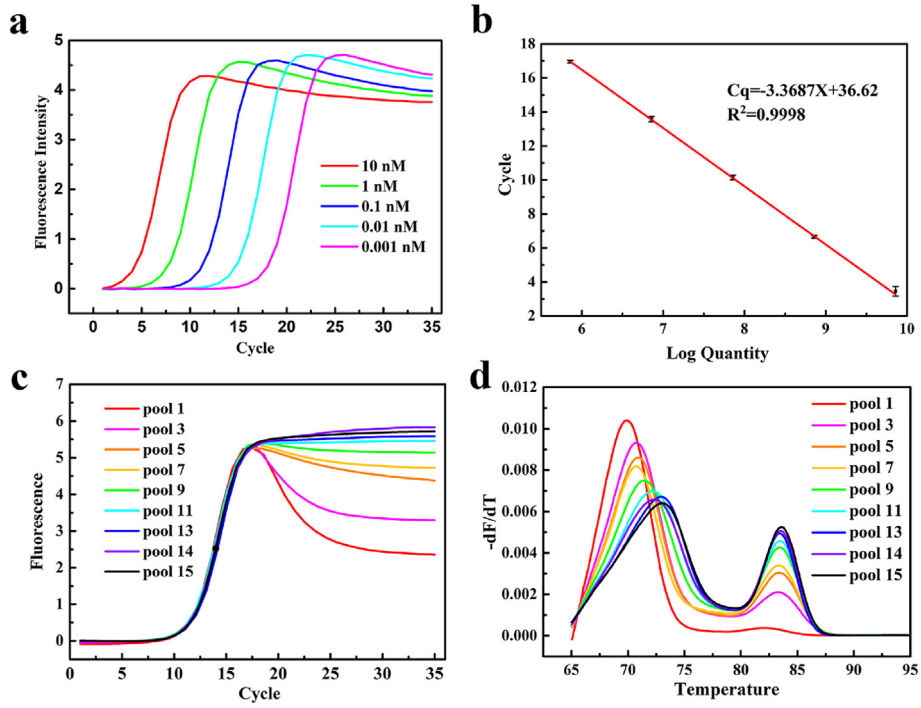

Fig. 2. (a) Q-PCR curves of libraries with different concentrations (10 nM, 1 nM, 0.1 nM, 0.01 nM, and 0.001 nM). (b) The linear correlation between the cycles and logarithm of molecular amount. (c) Amplification curve and (d) melting curve for 15 rounds of selection.

fluorescence was quenched (Fig. 3, blue curve). In the presence of phoxim, the aptamer-target and CS1-CS2-AuNPs stable structure were respectively formed in the solution, and the CS3-FAM was dissociated, and the fluorescence signal was released (Fig. 3, red curve). The higher the concentration of phoxim was, the freer was CS3-FAM in solution, and stronger was the fluorescence signal.

3.4. Analytical performance of aptasensor

Phoxim was diluted to different concentrations (0.01–60 μM), and the fluorescence spectrum is shown in Fig. 4a. The fluorescence intensity in the aptasensor increased with increased target concentration, and the target of each concentration had good dispersion in the diagram. Fig. 4b shows fluorescence intensity scatter diagram of phoxim with different

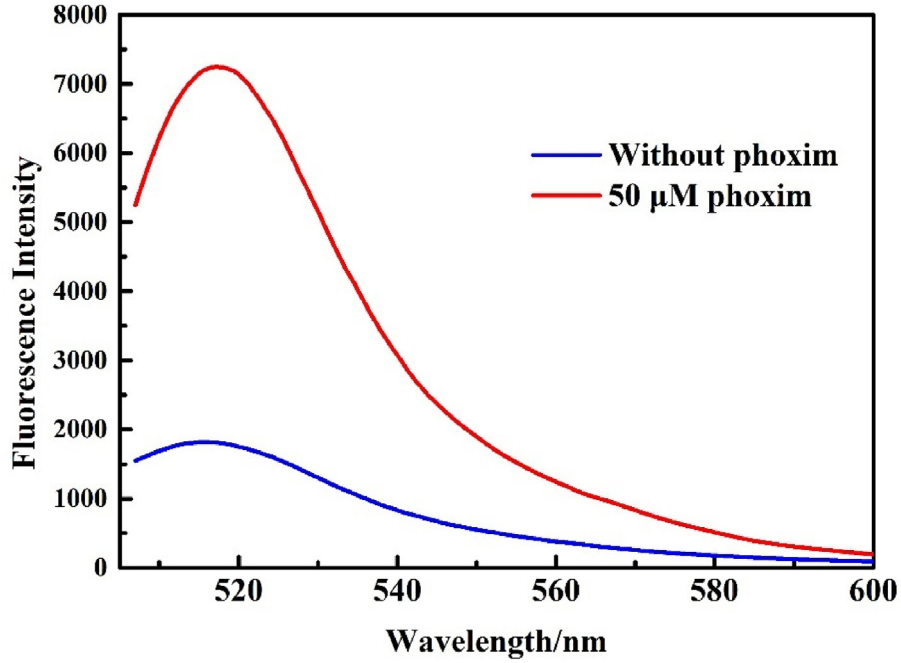

Fig. 3. Fluorescence intensity with or without phoxim in the sensor. In the absence of phoxim, the fluorescence signal was quenched (blue line). In the presence of phoxim, the fluorescence signal was released (red line).

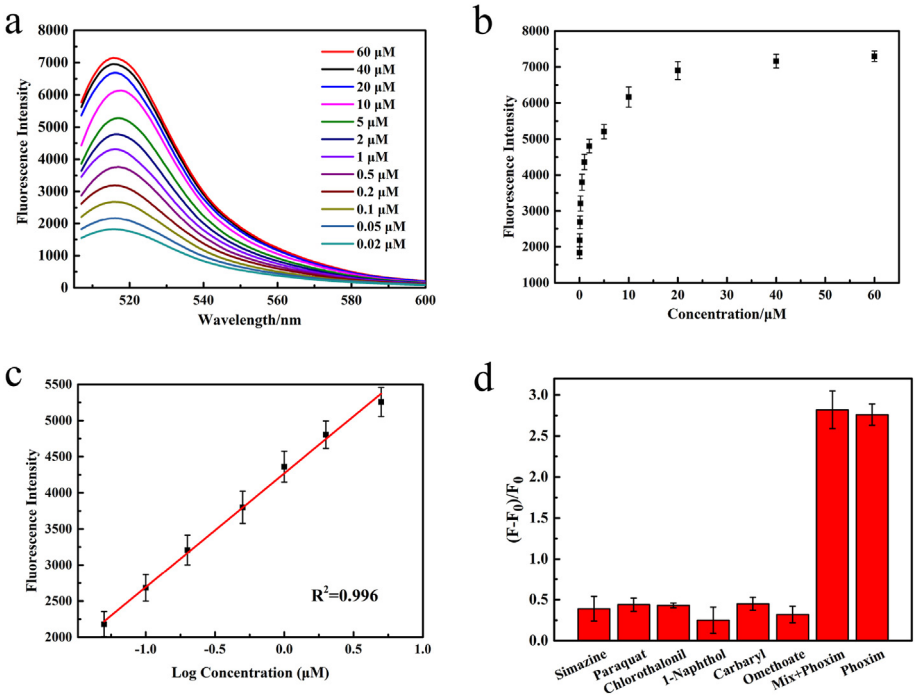

Fig. 4. (a) Fluorescence spectra of sensor in detecting different concentrations of phoxim (0.2–60 μM). (b) Scatter diagram of fluorescence intensity with different concentrations of phoxim. (c) The linear correlation between fluorescence intensity and phoxim concentration at 0.05–5 μM, $R^2 = 0.996$. (d) The specificity of aptasensor for phoxim comparing with its analogues. In the presence of phoxim, the sensor showed high fluorescence intensity.

concentrations. K_d was 0.93 ± 0.25 μM by nonlinear fitting according to the formula $F - F0 = \frac{Fmax \times X}{Kd+X}$, where F_0 was the fluorescence intensity without phoxim and X was the concentration of phoxim.

As shown in Fig. 4c, the aptasensor showed good linear relationship between the fluorescence intensity and concentration of phoxim in the range of 0.05–5 μM, and the linear equation was $F = 1576.53 \times \log C + 4269.63$ ($R^2 = 0.996$). According to the formula $LOD = \frac{3 \times SB}{S}$, the LOD was 29.69 nM, where S_B was the standard deviation of 12 independent blank samples and S was sensitivity. The detection results of 12 independent blank samples were shown in Fig. S3 (Supporting information), and the fluorescence spectrum curves almost coincide. The results showed that this sensor has good stability and repeatability.

The reported sensors were mainly based on polymer materials and enzymes, as shown in Table 3. The sensors based on polymer materials had low specificity and accuracy, and it was difficult to capture targets

Table 3
Phoxim detection in different manuscripts.

Materials	Type	Linear range	LOD
Acetylcholinasterase–AuNPs–silk fibroin composite [38]	Electrochemical sensor	5–200 nM	2 nM
Fluorescent carbon dots-AgNPs [39]	Colorimetric sensor	0.1–100 μM	0.04 μM
Poly(3-methylthiophene)/nitrogen doped graphene [40]	Electrochemical sensor	0.02–0.2 μM 0.2–20 μM	6.4 nM
Calix [4]arene-modified Si surface [41]	Visual sensor	Not reported	1 μM
High-luminescence perovskite quantum dots [42]	Fluorescence sensor	5–100 ng/mL	1.45 ng/mL
Gold nanoelectrode ensembles [43]	Electrochemical sensor	59–12000 μM	4.8 μM
Reduced graphene oxide-gold nanocomposite [44]	Electrochemical sensor	0.01–10 μM	3 nM
Ethylene glycol maleic rosinate acrylate [45]	Electrochemical sensor	0.8–140 μM	20 nM
4-(diethoxyphosphorothioylamino) butanoic acid/FPIA [46]	Fluorescence sensor	5.9–89.8 ng/mL	3.27 ng/mL
This work	Fluorescence aptasensor	0.05–5 μM	29.69 nM

accurately. Enzyme-based sensors had some disadvantages, such as complex preparation, high cost and poor repeatability, which affected the accuracy of the sensor. Compared with other reported sensors for phoxim detection, the aptasensor, as a fluorescence sensor, not only had the advantages of simple preparation and low cost, but also had high sensitivity, good linearity.

3.5. Selectivity of aptasensor

In order to test the specificity of the sensor, the sensor was applied for detection of analogues, such as simazine, paraquat, chlorothalonil, 1-naphthol, carbaryl, and omethoate. As shown in Fig. 4d, the fluorescence intensity of phoxim was much higher than that of analogues. F_0 was the fluorescence intensity in the blank solution, and concentration of pesticides was10 μM. Using the sensor to detect the mixture of phoxim and other pesticides, the fluorescence intensity obtained was similar to phoxim solution. The results herein demonstrated that the sensor had good specificity for phoxim.

3.6. Detection of phoxim in real samples

To verify the practical application value of the aptasensor, real samples were detected through the spiked recovery method. The sensor was used to detect three concentrations in Hunan Xiangjiang River and the results are listed in Table 4. The recovery of phoxim in the different solutions for each sample lay in the range of 95–110%, and all the relative standard deviations (RSD) did not exceed 3.0%. According to the latest "Effluent standards of pollutants for pesticides industry" in China, the emission limit of phoxim was 0.5 mg/L. Therefore, this sensor can meet the detection requirements and LOD was two orders of magnitude higher than the limit. These results show that this aptasensor can detect phoxim accurately and can be applied in practical detection.

Table 4
Determination of phoxim in real samples.

Sample	Added Phoxim (μM)	Total Found (μM)	Recovery (%)	RSD (n = 3, %)
Xiangjiang River	0.5	0.537	107.4	2.3
Xiangjiang River	1.0	0.951	95.1	1.3
Xiangjiang River	2.0	1.986	99.3	1.8

4. Conclusion

In summary, phoxim aptamer with K_d of 0.93 ± 0.25 μM was in this study successfully obtained by MB-SELEX technique, Q-PCR quantitative method and AC-MAC monitoring method. This method was generally suitable for aptamer selection of small molecules such as heavy metals and pesticides. Then, using the obtained aptamer, the fluorescent aptasensor applying multi-complementary strands structure and AuNPs (as quenching agent) was constructed. The extinction coefficient of AuNPs was much higher than that of organic quenching agents, and was able to reduce the background signal of the sensor. The full combination of target and aptamer in solution could reduce the influence of steric hindrance and environmental factors on the sensor. The addition of multiple complementary strands stabilized the existing aptamer-target complex and dsDNA structure in the solution, and further improved the stability of the sensor. The introduction of independent fluorescent and quenching chains could avoid the potential effects on the aptamer structure due to modification groups. Therefore, the multi-complementary strands structure effectively improved the stability and sensitivity of the aptasensor. The results herein showed that the linear range of the sensor for phoxim was 0.05–5 μM ($R^2 = 0.996$), and LOD was 29.69 nM. In the detection of real samples of Hunan Xiangjiang River, it was proved that the aptamer has promising application prospect.

CRediT authorship contribution statement

Wenfei Guo: Writing – original draft. **Dan Wei:** Part Experiment. **Franklin Wang-Ngai Chow:** Experiment design. **Polly Hang-Mei Leung:** Experiment design. **Hanming Wang:** Validation. **Lei Cai:** Part Experiment. **Masahi Hori:** Writing – review & editing. **Zhu Chen:** Experiment design. **Song Li:** Writing – review & editing. **Yan Deng:** Supervision.

Declaration of competing interest

The authors declare that they have no known competing financial interests or personal relationships that could have appeared to influence the work reported in this paper.

Acknowledgments

This work was financially supported by the National Key Research and Development Program of China (No. 2018YFC1602905), China. The National Natural Science Foundation of China (61871180, 61971187, and 61901168), China.

Appendix A. Supplementary data

Supplementary data to this article can be found online at https://doi.org/10.1016/j.smaim.2022.03.003.

References

[1] U. Bajwa, K.S. Sandhu, Effect of handling and processing on pesticide residues in food- a review, J. Food Sci. Technol. 51 (2014) 201–220.
[2] D. Wang, C. Liu, Z. Zhou, P. Wang, Recent advances in rapid detection of pesticide residues, Chin. J. Pesticide Sci. 21 (2019) 852–864.
[3] J.S. Noori, J. Mortensen, A. Geto, Recent development on the electrochemical detection of selected pesticides: a focused review, Sensors 20 (2020) 2221.
[4] L. Yao, P. Dai, L. Ouyang, L. Zhu, A sensitive and reproducible SERS sensor based on natural lotus leaf for paraquat detection, Microchem. J. 160 (2021) 105728.
[5] M. Liu, A. Khan, Z. Wang, Y. Liu, G. Yang, Y. Deng, N. He, Aptasensors for pesticide detection, Biosens. Bioelectron. 130 (2019) 174–184.
[6] D. Su, H. Li, X. Yan, Y. Lin, G. Lu, Biosensors based on fluorescence carbon nanomaterials for detection of pesticides, TrAC Trends Anal. Chem. (Reference Ed.) 134 (2021) 116126.

[7] P. Liu, J. Zhang, Progress on detection methods for organophosphorus pesticide studies, Environ. Technol. Control 28 (2006) 55–57.
[8] Jyoti, C. Gonzato, T. Zolek, D. Maciejewska, A. Kutner, F. Merlier, K. Haupt, P.S. Sharma, K.R. Noworyta, W. Kutner, Molecularly imprinted polymer nanoparticles-based electrochemical chemosensors for selective determination of cilostazol and its pharmacologically active primary metabolite in human plasma, Biosens. Bioelectron. 193 (2021) 113542.
[9] J. Wang, L. Zou, J. Xu, R. Zhang, H. Zhang, Molecularly imprinted fluoroprobes doped with Ag nanoparticles for highly selective detection of oxytetracycline in real samples, Anal. Chim. Acta 1161 (2021) 338326.
[10] C. Li, J. Ma, H. Shi, X. Hu, Y. Xiang, Y. Li, G. Li, Design of a stretchable DNAzyme for sensitive and multiplexed detection of antibodies, Anal. Chim. Acta 1041 (2018) 102–107.
[11] Y. Li, G. Jin, L. Liu, H. Kuang, J. Xiao, C. Xua, A portable fluorescent microsphere-based lateral flow immunosensor for the simultaneous detection of colistin and bacitracin in milk, Analyst 145 (2021) 7884–7892.
[12] G. Zhao, H. Wang, G. Liu, Advances in biosensor-based instruments for pesticide residues rapid detection, Int. J. Electrochem. Sci. 10 (2015) 9790–9807.
[13] R. Cai, H. Xiang, D. Yang, K.-T. Lin, Y. Wu, R. Zhou, Z. Gu, L. Yan, Y. Zhao, W. Tan, Plasmonic AuPt@CuS heterostructure with enhanced synergistic efficacy for radiophotothermal therapy, J. Am. Chem. Soc. 143 (2021) 16113–16127.
[14] S. Epple, A. Modi, Y.R. Baker, E. Wegrzyn, D. Traore, P. Wanat, A.E.S. Tyburn, A. Shivalingam, L. Taemaitree, A.H. El-Sagheer, T. Brown, A New 1,5-Disubstituted triazole DNA backbone mimic with enhanced polymerase compatibility, J. Am. Chem. Soc. 143 (2021) 16293–16301.
[15] Y. Liu, M. Klement, Y. Wang, Y. Zhong, B. Zhu, J. Chen, M. Engel, X. Ye, Macromolecular ligand engineering for programmable nanoprism assembly, J. Am. Chem. Soc. 143 (2021) 16163–16172.
[16] C.P. Kurup, C. Tlili, S.N.A. Zakaria, M.U. Ahmed, Recent trends in design and development of nanomaterial-based aptasensors, Biointerface Res. Appl. Chem. 11 (2021) 14057–14077.
[17] T. Wang, C. Chen, L.M. Larcher, R.A. Barrero, R.N. Veedu, Three decades of nucleic acid aptamer technologies: lessons learned, progress and opportunities on aptamer development, Biotechnol. Adv. 37 (2019) 28–50.
[18] J. Yan, H. Xiong, S. Cai, N. Wen, Q. He, Y. Liu, D. Peng, Z. Liu, Advances in aptamer screening technologies, Talanta 200 (2019) 124–144.
[19] A. Boussebayle, F. Groher, B. Suess, RNA-based Capture-SELEX for the selection of small molecule-binding aptamers, Methods 161 (2019) 10–15.
[20] M.M. Zourob, S.H.H. Eissa, Selection and characterization of DNA aptamers for electrochemical biosensing of carbendazim, Anal. Chem. 89 (2017) 3138–3145.
[21] Y. Zhang, B.S. Lai, M. Juhas, Recent advances in aptamer discovery and applications, Molecules 24 (2019) 941.
[22] F. Cao, X. Lu, X. Hu, Y. Zhang, L. Zeng, L. Chen, M. Sun, In vitro selection of DNA aptamers binding pesticide fluoroacetamide, Biosci. Biotechnol. Biochem. 80 (2016) 823–832.
[23] W. Guo, C. Zhang, T. Ma, X. Liu, Z. Chen, S. Li, Y. Deng, Advances in aptamer screening and aptasensors' detection of heavy metal ions, J. Nanobiotechnol. 19 (2021) 166.
[24] L. Gao, H. Wang, Z. Deng, W. Xiang, H. Shi, B. Xie, H. Shi, Highly sensitive detection for cocaine using an aptamer–cocaine–aptamer method, New J. Chem. 44 (2020) 2571–2577.
[25] N. Komarova, M. Andrianova, S. Glukhov, A. Kuznetsov, Selection, characterization, and application of ssDNA aptamer against furaneol, Molecules 23 (2018) 3159.
[26] R.V. Nair, P.R. Chandran, A.P. Mohamed, S. Pillai, Sulphur-doped graphene quantum dot based fluorescent turn-on aptasensor for selective and ultrasensitive detection of omethoate, Anal. Chim. Acta 1181 (2021) 338893.
[27] A. Bahreyni, H. Luo, M. Ramezani, M. Alibolandi, V. Soheili, N.M. Danesh, M.S. Ashjaei, K. Abnous, S.M. Taghdisi, A fluorescent sensing strategy for ultrasensitive detection of oxytetracycline in milk based on aptamer-magnetic bead conjugate, complementary strand of aptamer and PicoGreen, Spectrochim. Acta Part A Mol. Biomol. Spectrosc. 246 (2021) 119009.
[28] Y. Chen, H. Li, T. Gao, T. Zhang, L. Xu, B. Wang, J. Wang, R. Pei, Selection of DNA aptamers for the development of light-up biosensor to detect Pb(II), Sensor. Actuator. B Chem. 254 (2018) 214–221.
[29] K.L. Hong, L.J. Sooter, In Vitro selection of a single-stranded DNA molecular recognition element against the pesticide fipronil and sensitive detection in river water, Int. J. Mol. Sci. 19 (2017) 14332.
[30] Y. Liu, G. Yang, T. Li, Y. Deng, Z. Chen, N. He, Selection of a DNA aptamer for the development of fluorescent aptasensor for carbaryl detection, Chin. Chem. Lett. 32 (2021) 1957–1962.
[31] A. Bahreyni, R. Yazdian-Robati, M. Ramezani, K. Abnous, S.M. Taghdisi, Fluorometric aptasensing of the neonicotinoid insecticide acetamiprid by using multiple complementary strands and gold nanoparticles, Microchim. Acta 185 (2018) 272.
[32] Q. Liu, H. Wang, P. Han, X. Feng, Fluorescent aptasensing of chlorpyrifos based on the assembly of cationic conjugated polymer-aggregated gold nanoparticles and luminescent metal-organic frameworks, Analyst 144 (2019) 6025–6032.
[33] W.-B. Tseng, M.-M. Hsieh, C.-H. Chen, T.-C. Chiu, W.-L. Tseng, Functionalized gold nanoparticles for sensing of pesticides: a review, J. Food Drug Anal. 28 (2020) 522–539.
[34] H. Wang, Y. Wang, J. Jin, R. Yang, Gold nanoparticle-based colorimetric and "Turn-on" fluorescent probe for mercury(II) ions in aqueous solution, Anal. Chem. 80 (2008) 9021–9028.
[35] O. Alkhamis, J. Canoura, H. Yu, Y. Liu, Y. Xiao, Innovative engineering and sensing strategies for aptamer-based small-molecule detection, TrAC Trends Anal. Chem. (Reference Ed.) 121 (2019) 115699.
[36] Z. Luo, L. He, J. Wang, X. Fang, L. Zhang, Developing a combined strategy for monitoring the progress of aptamer selection, Analyst 142 (2017) 3136–3139.
[37] S.K. Ghosh, T. Pa, Interparticle coupling effect on the surface plasmon resonance of gold nanoparticles: from theory to applications, Chem. Rev. 107 (2007) 4797–7862.
[38] H. Yin, S. Ai, J. Xu, W. Shi, L. Zhu, Amperometric biosensor based on immobilized acetylcholinesterase on gold nanoparticles and silk fibroin modified platinum electrode for detection of methyl paraoxon, carbofuran and phoxim, J. Electroanal. Chem. 637 (2009) 21–27.
[39] M. Zheng, C. Wang, Y. Wang, W. Wei, S. Ma, X. Sun, J. He, Green synthesis of carbon dots functionalized silver nanoparticles for the colorimetric detection of phoxim, Talanta 185 (2018) 309–315.
[40] L. Wu, W. Lei, Z. Han, Y. Zhang, M. Xia, Q. Hao, A novel non-enzyme amperometric platform based on poly(3-methylthiophene)/nitrogen doped graphene modified electrode for determination of trace amounts of pesticide phoxim, Sensor. Actuator. B Chem. 206 (2015) 495–501.
[41] J. Feng, G. Yang, Y. Mei, X. Cao, Y. Wang, H. Li, Q. Lu, Macroscopic visual detection of phoxim by calix[4]arene-based host-guest chemistry, Sensor. Actuator. B Chem. 271 (2018) 264–270.
[42] L. Tan, M. Guo, J. Tan, Y. Geng, S. Huang, Y. Tang, C. Su, C. Lin, Y. Liang, Development of high-luminescence perovskite quantum dots coated with molecularly imprinted polymers for pesticide detection by slowly hydrolysing the organosilicon monomers in situ, Sensor. Actuator. B Chem. 291 (2019) 226–234.
[43] X. Lu, H. Bai, Q. Ruan, M. Yang, G. Yang, L. Tan, Y. Yang, Direct determination of pesticides in vegetable samples using gold nanoelectrode ensembles, Int. J. Environ. Anal. Chem. 88 (2008) 813–824.
[44] Y. Zheng, A. Wang, H. Lin, L. Fu, W. Cai, A sensitive electrochemical sensor for direct phoxim detection based on an electrodeposited reduced graphene oxide–gold nanocomposite, RSC Adv 5 (2015) 15425–15430.
[45] X. Tan, J. Wu, Q. Hu, X. Li, P. Li, H. Yu, X. Li, F. Lei, An electrochemical sensor for the determination of phoxim based on a graphene modified electrode and molecularly imprinted polymer, Anal. Methods 7 (2015) 4786–4792.
[46] Z.-L. Xu, Q. Wang, H.-T. Lei, S.A. Eremin, Y.-D. Shen, H. Wang, R.C. Beier, J.-Y. Yang, K.A. Maksimova, Y.-M. Sun, A simple, rapid and high-throughput fluorescence polarization immunoassay for simultaneous detection of organophosphorus pesticides in vegetable and environmental water samples, Anal. Chim. Acta 708 (2011) 123–129.